ISSN:0975-3583,0976-2833 VOL8,ISSUE04,2017

Vibrational Spectroscopic Analysis of 4-amino-3-(4-chlorophenyl)-butanoic acid by Density Functional method

T.Jayaprakash[1], K.Parimala Gandhi [2], G.Rajeshkanna[3], R.Saravanakumar[4],N.Mohan[5]J. Ashok[6] and M. Jeganathan[7]

[1-5]Department of Science and Humanities, Nehru Institute of Technology,Coimbatore.

[6]Dean, Dhanalakshmi srinivasan School of Architecture, Perambalur - 621113.

[7]Associate Professor,Designed Environment and Research Institute (DEAR Institute) Trichy- 621 213.

nitparimalagandhi@nehrucolleges.com

Abstract

4-amino-3-(4-chlorophenyl)-butanoicacid(4ACBA) otherwise commonly called as Baclofen is a drug used for the treatment of alcohol dependence The solid phase FT-IR and FT-Raman spectra of Baclofen were recorded in the regions 4000–400 cm^{-1} and 3500–100 cm^{-1} respectively. Theoretical vibrational frequencies , geometric parameters (bond lengths and bond angles),Thermodynamic properties,frequency and intensity of the vibrational bands , Natural population analysis and Mulliken atomic charges of Baclofen were obtained by the Restricted Hartree–Fock (RHF) density functional theory (DFT) with complete relaxation in the potential energy surface using 6-31G(d,p) basis set.The harmonic vibrational frequencies for Baclofen were calculated and the scaled values have been compared with experimental values of FTIR and FT-Raman spectra. The observed and the calculated frequencies are found to be in good agreement. Stability of the molecule arising from hyperconjugative interactions and charge delocalization has been analyzed using natural bond orbital (NBO) analysis. The electronic dipole moment (lD) and the first hyperpolarizability (β_{tot}) values of the investigated molecule were computed using Density Functional Theory (DFT/B3LYP) and HF with 6-31+G(d,p) basis sets.The calculated results also show that the (4ACBA) molecule may have microscopy nonlinear optical (NLO) behavior with non zero values. ^{1}H and ^{13}C NMR spectra were recorded and^{1}H and ^{13}C nuclear magnetic resonance chemical shift of the molecule were calculated using thegauge independent atomic orbital (GIAO) method.

1.Introduction

Alcoholism is a primary, chronic disease with genetic, psychosocial, and environmental factors influencing its development and manifestations. The disease is often progressive and fatal. It is characterized by impaired control over drinking, preoccupation with the drug alcohol, use of alcohol despite adverse consequences, and distortions in thinking, most notably denial. Each of these symptoms may be continuous or periodic." This definition recognizes alcoholism as a disease, i.e., as an involuntary disability. It accepts a genetic vulnerability in some people and identifies the phenomenon of denial as both a psychological defense mechanism and a physiologicaloutcome of alcohol's effect on the memory.It is medically considered a disease,

ISSN:0975-3583,0976-2833 VOL8,ISSUE04,2017

specifically an addictive illness, and in psychiatry several other terms are used, specifically "alcohol abuse" and "alcohol dependence," which have slightly different definitions[1].Identifying alcoholism is difficult for the individual afflicted because of the social stigma associated with the disease that causes people with alcoholism to avoid diagnosis and treatment for fear of shame or social consequences. The evaluation responses to a group of standardized questioning are a common method for diagnosing alcoholism. These can be used to identify harmful drinking patterns, including alcoholism[2].Baclofen (brand names Kemstro, Lioresal, Liofen, Gablofen, Lyflex, Beklo and Baclosan) is a derivative ofgamma-aminobutyric acid (GABA). It is primarily used to treat spasticity and is in the early research stages for use for the treatment of alcoholism. It is also used by compounding pharmacies in topical pain creams as a muscle relaxant.It is an agonist for the $GABA_B$ receptors[3,4]. Its beneficial effects in spasticity result from actions at spinal andsupraspinal sites. Baclofen can also be used to treat hiccups, and has been shown to prevent rises in body temperature induced by the drug MDMA in rats[5].Baclofen is also usedto treat muscle spasms caused by certain conditions (such as multiple sclerosis, spinal cord injury/disease). It works by helping to relax the muscles.Converging evidence suggest that the gamma-aminobutyric acid-B receptor agonist baclofen is a promising agent for the treatment of alcoholism.Baclofen side effects include drowsiness, weakness, dizziness, headache, seizures, nausea, vomiting, low blood pressure, constipation, confusion, respiratory depression, insomnia, and increased urinary frequency or urinary retention. Abrupt discontinuation of baclofen may cause seizures and hallucinations, high fever, rebound spasticity, muscle rigidity, and rhabdomyolysis.Baclofen is a white (or off white) mostly odorless crystalline powder, with a molecular weight of 213.66 g/mol. It is slightly soluble in water, very slightly soluble inmethanol, and insoluble in chloroform. Baclofen Tablets USP 10 mg and 20 mg contain the following inactive ingredients: magnesiumstearate, microcrystalline cellulose, povidone and starch (corn).It is manufactured by LANNETT COMPANY, INC**.**Philadelphia, PA 19136 Made in the USA.(Vasanthy and Jeganathan 2007, Vasanthy et.al., 2008, Raajasubramanian et.al., 2011, Jeganathan et.al., 2012, 2014, Sridhar et.al., 2012, Gunaselvi et.al., 2014, Premalatha et.al., 2015, Seshadri et.al., 2015, Shakila et.al., 2015, Ashok et.al., 2016, Satheesh Kumar et.al., 2016).

2. Experimental details

The pure compound 4ACBA was purchased from USA with more than 98% purity and was used as such without further purification to record FTIR and FT Raman spectra.The FTIR spectrum of the compound is recorded in the region 4000–400 cm^{-1} in evacuation mode on Bruker IFS 66V spectrophotometer using KBr pellet technique (solid phase) with 4.0 cm^{-1} resolution. The FT Raman spectrum is recorded using 1064 nm line of Nd:YAG laser as excitation wavelength in the region 3500–100 cm^{-1}on Bruker IFS 66V spectrometer equipped with FRA 106 FT Raman module accessory. The spectral measurements were carried out at Sophisticated Instrumentation Analysis Facility, IIT,Madras,India. The experimental FTIR and FT Raman spectra of CAS are presented in the Figs.1and 2.

ISSN:0975-3583,0976-2833 VOL8,ISSUE04,2017

3. Computational methods

In the present work, the density functional method (DFT) [6] has been employed using Becke's three parameter hybrid exchange functional [11] with the Lee–Yang–Parr correlation functional [7,8] to optimize the structure of the molecule and also to calculate the electronic structure of the title molecule. The entire calculations were performed at ab initio HartreeFock (HF) and DFT method using B3LYP levels at 6-31+G(d,p) basis sets on a Pentium V/1.6 GHz personal computer by using Gaussian 03W program package [9,10] and applied geometry optimization [11]. Initial geometry generated, was minimized at the HartreeFock level using 6-31+G(d,p) basis set and also optimized at DFT/B3LYP levels at 6-31+G(d,p) basis set. The vibrational modes are assigned using Gauss-View molecular visualization program package. The optimized structural parameters were used in the vibrational frequency calculations at the DFT levels to characterize all stationary points as minima. The vibrational frequencies were calculated and scaled down by the appropriate scaling factor and thereby the vibrational assignments are compared with observed values.Furthermore, in order to show nonlinear optics (NLO) activity of title molecule, the dipole moment, linear polarizability and first hyper polarizability were obtained.The natural bonding orbital (NBO) calculations[12] were performed using NBO 3.1 program as implemented in the Gaussian 03W package at the above said level in order to understand various second order interactions between the filled orbital of one subsystem and vacant orbital of another subsystem, which is a measure of the intermolecular and intramolecular delocalization or hyper conjugation. The molecular geometry was not restricted and all the calculations (vibrational wave numbers,geometric parameters and other molecular properties) wereperformed by using Gauss View molecular visualization program [13] and Gaussian 03 program package on a computing system [14].(Manikandan et.al., 2016, Sethuraman et.al., 2016, Senthil Thambi et.al., 2016).

Results and discussion

4.Molecular geometry

The optimized structure parameters of 4ACBA are calculated by DFT and HF level with 6-31+G(d,p) basis set shown in Table.1in accordance with the atom numbering scheme given in Fig.3.The comparative optimized structural parameters such as bond length, bond angle along with its experimental datas are presented in Table.1. The molecule has 26 atoms and 72 normal modes of fundamental vibrations. All the 72 vibrations are active in both IR and Raman.A general priority for reproducing the experimental bond lengths and bond angles [15] is not present among HF and DFT levels.All calculated geometrical parameters obtained at the DFT level of theory are in good agreement with the experimental structural parameters. The molecule has 10 C-C bond lengths, 2 C-O and N-H bond lengths, nine C-H bond lengths ,one C-N,O-H,C-CL bond lengths.The C-C bond lengths in the optimized geometry of 4ACBAcalculated at both levels fall in the range; 1.394–1.515 Å.It is close agreement with the experimental values [16]. A similar trend has also been observed in the case of the C-N, O-H,C-CL bonds. The nine C-H lengths (1.113 Å) are almost equal at B3LYP/6-31+G(d,p) basis set.

From theoretical values, we found most of the optimized bond lengths are in good agreement with experimental bonds lengths, but bond angles are slightly longer and shorter than that of experimental values.

ISSN:0975-3583,0976-2833 VOL8,ISSUE04,2017

5.Vibrational assignments

IR and Raman spectra contain a number of bands at specific wavenumbers. The aim of the vibrational analysis is to decide which of the vibrational modes give rise to each of these observed bands. According to the theoretical calculations, 4ACBA has a structure of C1 point groupsymmetry.The molecule has 26 atoms and 72 normal modes of fundamental vibrations (3N-6).A satisfactory vibrational band assignment has been done.Almost all the 72 fundamental vibrations are active in both IR absorption and Raman scattering.The frequencies of fundamental vibrational modes together with intensities calculated on the basis of HF and DFT methods are tabulated in Table 2.Chemcraft [17], a graphical interface, was used to assign the calculated harmonic wavenumbers using scaled displacement vectors to identify the motion of modes.On the whole, the predicted vibrational wavenumbers are in agreement with the experimental results.

C–NH_2 vibrations

The molecule under investigation possesses only one NH_2 group and hence one expects one symmetric and one asymmetric N– H stretching vibrations in NH_2group. In all the primary aromatic amines, the N–H stretching frequency occurs in the region 3300–3500cm^{-1}[18]. The asymmetric- NH_2 stretching vibration appears from 3500 to 3420 cm^{-1} and the symmetric- NH_2 stretching is observed in the range 3420– 3340 cm^{-1} [19].Hence, the band in IR spectrum were located at 3307 cm^{-1} and Raman spectrum were located at 3275 cm^{-1} are assigned toN–H symmetric and asymmetric stretching vibrations, respectively in NH_2 group. These assignments agree well with the earlier reports[20].The scaled NH_2 symmetric and asymmetric stretching are in the range of 3308–3278 cm^{-1} in B3LYP/6-31+G(d,p).The various vibrations NH_2group of the title compound are also found to be in good agreement with the experimental values.

C-H vibration

The existence of one or more aromatic rings in a structure is normally readily determined from the C-H and C-C ring related vibrations. The substituted benzene like molecule gives rise to C-H stretching, C-H in-plane and C-H out-of-plane bending vibrations.Thehetro aromatic structure shows the presence of C-H stretching vibration in the region 3100–3000 cm^{-1} , which is the characteristic region for the ready identification of C-H stretching vibration [21,22]. In this region, the bands are not affected appreciably by the nature of the substituent. The aromatic C-H stretching frequencies arise from the modes observed at 3062, 3047 cm^{-1} and 3080 cm^{-1} of benzene and its derivatives[23].In our present work,the C-H stretching vibrations are observed at 2907 cm^{-1} in FT-Raman spectrum for C-H vibrations.The calculated values of these modes for the title molecule have been found to be 2820 cm^{-1} and 2911 cm^{-1} at HF and B3LYP calculation level.In general the aromatic C–H stretching vibrations calculated theoretically are in good agreement with the experimentally values.

C–C Vibrations

The carbon–carbon stretching modes of the phenyl group are expected in the range from 1650 to 1200 cm^{-1}. The actual position of these modes is determined not so much by the nature of thesubstituent but by the form of substitution around the ring [24]. In general, the bands are of variable intensity and are observed at 1625–1590, 1590–1575, 1540–1470, 1465–1430 and

ISSN:0975-3583,0976-2833 VOL8,ISSUE04,2017

1380– 1280 cm^{-1} from the frequency ranges given by Varsanyi [25] for the five bands in the region. In the present work, the wave numbers observed in the FTIR spectrum at 1489,1400 cm^{-1} and FT-Raman spectrum 1460,1437,1413 cm^{-1} have been assigned to C-C stretching vibrations.

CH_2 group vibrations

For the assignments of CH_2 group frequencies, basically six fundamentals can be associated to each CH2 group namely CH_2 symmetric stretch; CH_2asymmetric stretch; CH_2 scissoring and CH_2 rocking which belongs to in plane vibrations and two out-of-plane vibrations, viz., CH_2 wagging and CH_2 twisting modes, which are expected to be polarized [26]. The asymmetrical CH_2 stretching vibrations are generally observed around 3000 cm^{-1} while the symmetric stretch will appear between 3000 and 2900 cm^{-1} region [27,28]. In this study, the asymmetric stretching vibrations are observed at 2975 cm^{-1} in FTIR and 2978 cm^{-1} in FT-Raman spectrum and symmetric stretching vibrations are observed at 2928,2912 cm^{-1} in FTIR and 3198,3063 cm^{-1} in the FT-Raman spectrum .These experimental values correlates well with the HF and B3LYP calculation level .

Deformation Vibrations

The C-C-C bending bands always occur below 700 cm^{-1}.Isopropyl benzenes [29,30] have a medium intensity absorption band in the region 545-525 $cm^{-1.}$.The C-C-C vibration is found at 671 cm^{-1} in the FT-IR spectrum and 668 cm^{-1} in the FT-Raman spectrum.This correlates well with the calculated values.

6. Natural population analysis

Population analysis is the study of charge distribution within molecules.The calculation of effective atomic charges plays an important role in the application of quantum mechanical calculations to molecular systems[31].Our interest here is in the comparison of different methods (RHF and DFT) to describe the electron distribution in 4ACBA is broadly as possible, and to assess the sensitivity of the calculated charges to changes in the choice of the quantum chemical method.The calculated atomic charge values from the natural population analysis (NPA) and Mulliken population analysis (MPA) procedures using the RHF and DFT methods are listed in Table 3.The charge distribution of 4ACBA is shown in Fig.4.The NPA from the natural bonding orbital (NBO) method is better than the MPA scheme. The NPA of 4ACBA shows the presence of Nitrogen atoms in the hydrogen moiety [N_6= -0.95433(DFT) and N_6= -0.99946(RHF)] imposes positive charges on the hydrogen atoms H_{25}=0.40392(DFT),H_{25}=0.40987(RHF) and H_{26}= 0.40375(DFT) , H_{26}= 0.41061(RHF). However the oxygen atom O_6 posses large negative charges, resulting in the positive charges on the C_1 and H_{20} atoms.Moreover, there is no differences in charge distribution observed on all hydrogen atoms except the H_{20},H_{25},H_{26} Hydrogen atoms.The large positive charge on these hydrogen atoms is due to the large negative charge accumulated on the N_{14} and O_6 atoms respectively.

7.Thermodynamic properties

Several calculated thermodynamic parameters such as,rotational constants, zero point thermal energy, specific heat capacity,entropy,dipolemoment,Gibbs free energy have been presented in

ISSN:0975-3583,0976-2833 VOL8,ISSUE04,2017

Table4.Scale factors have been recommended [32] for accurate reductions in determining the Zero-Point Vibration Energies (ZPVEs) and the entropy, the variations in the PVEs seem to be significant.The total energies and the change in the total entropy of 4ACBA at room temperature by different methods are also presented in Table 4.The change in the Gibbs free energy of4ACBA at room temperature for both the methods are only marginal.The highest value of ZPVE of 4ACBA is 140.634 kcal mol^{-1} obtained by HF/6-31+G(d,p), whereas the lowest one is 130.955 kcal mol^{-1}, obtained by B3LYP/6-31+G(d,p) method. Dipole moment reflects the molecular charge distribution and is given as a vector in three dimensions. Therefore, it can be used as an illustrator to depict the charge movement across the molecule. As a result, the dipole moment of 4ACBA was observed at 2.3931D in HF/6-31+G(d,p) method whereas 3.4111D in B3LYP/6-31+G(d,p)method.

8. NLO properties

The first hyperpolarizability (β_0) of this novel molecular system and related properties (β_{tot}, α,$\Delta\alpha$) of 4ACBA are calculated using DFT/B3LYP methods at 6-31+G(d,p) basis set based on the finite field approach. In the presence of an applied electric field, the energy of a system is a function of the electric field. First, hyperpolarizability is a third-rank tensor that can be described by a 3x 3 x 3 matrix. The 27 components of the 3D matrix can be reduced to 10 components due to the Kleinman symmetry [33]. It can be given in the lower tetrahedral format. It is obvious that the lower part of the 3x 3 x 3 matrixes is a tetrahedral. The components of β are defined as the coefficients in the Taylor series expansion of the energy in the external electric field. When the external electric field is weak and homogeneous, the expansion becomes

$$E = E^0 - \mu_x F_\alpha - 1/2\alpha_{\alpha\beta} F_\alpha F_\beta - 1/6\beta_{\alpha\beta\gamma} F_\alpha F_\beta F_\gamma + \ldots\ldots$$

where E^0 is the energy of the unperturbed molecules, F_α is the field at the origin and μ_x ,$\alpha_{\alpha\beta}$and $\beta_{\alpha\beta\gamma}$are the components of dipole oment,polarizability and the first hyperpolarizabilitiesrespectively.The total static dipole moment μ_D, the mean polarizability α, the anisotropy of the polarizability $\Delta\alpha$ and the mean first hyperpolarizabilityβ_{tot} using the x, y, z components, they are defined as

$$\mu_D = (\mu^2_x + \mu^2_y + \mu^2_z)^{1/2}$$

$$\alpha = \frac{\alpha_{xx} + \alpha_{yy} + \alpha_{zz}}{3}$$

$$\Delta\alpha = 2^{-1/2}[(\alpha_{xx} - \alpha_{yy})^2 + (\alpha_{yy} - \alpha_{zz})^2 + (\alpha_{zz} - \alpha_{xx})^2 + 6\,\alpha^2 xx]^{1/2}$$

$$\beta_{tot} = (\beta^2_x + \beta^2_y + \beta^2_z)^{1/2} \text{ and}$$

$$\beta_x = \beta_{xxx} + \beta_{xyy} + \beta_{xzz}$$

$$\beta_y = \beta_{yyy} + \beta_{xxy} + \beta_{yzz}$$

$$\beta_z = \beta_{zzz} + \beta_{xxz} + \beta_{yyz}$$

ISSN:0975-3583,0976-2833 VOL8,ISSUE04,2017

The calculation of the total molecular dipole moment (μ_D), linear polarizability (α) and first hyperpolarizability (β_{tot}) from the Gaussian output have been explained in detail previously [34],and DFT has been extensively used as an effective method to investigate the organic NLO materials [35–39]. In addition, the polar properties and dipole moment of the title compound were calculated at the B3LYP/6-31G (d,p) level using Gaussian 03W program package.

$$E = E^0 - \mu_x F_\alpha - 1/2\alpha_{\alpha\beta} F_\alpha F_\beta - 1/6\beta_{\alpha\beta\gamma} F_\alpha F_\beta F_\gamma + \ldots\ldots$$

where E^0 is the energy of the unperturbed molecules, F_α is the field at the origin and μ_x ,$\alpha_{\alpha\beta}$and $\beta_{\alpha\beta\gamma}$are the components of dipole oment,polarizability and the first hyperpolarizabilitiesrespectively.The total static dipole moment μ_D, the mean polarizability α, the anisotropy of the polarizability $\Delta\alpha$ and the mean first hyperpolarizabilityβ_{tot} using the x, y, z components, they are defined as

$$\mu_D = (\mu^2_x + \mu^2_y + \mu^2_z)^{1/2}$$

$$\alpha = \frac{\alpha_{xx} + \alpha_{yy} + \alpha_{zz}}{3}$$

$$\Delta\alpha = 2^{-1/2} [(\alpha_{xx} - \alpha_{yy})^2 + (\alpha_{yy} - \alpha_{zz})^2 + (\alpha_{zz} - \alpha_{xx})^2 + 6\alpha^2 xx]^{1/2}$$

$$\beta_{tot} = (\beta^2_x + \beta^2_y + \beta^2_z)^{1/2} \text{ and}$$

$$\beta_x = \beta_{xxx} + \beta_{xyy} + \beta_{xzz}$$

$$\beta_y = \beta_{yyy} + \beta_{xxy} + \beta_{yzz}$$

$$\beta_z = \beta_{zzz} + \beta_{xxz} + \beta_{yyz}$$

The calculation of the total molecular dipole moment (μ_D), linear polarizability (α) and first hyperpolarizability (β_{tot}) from the Gaussian output have been explained in detail previously [50],and DFT has been extensively used as an effective method to investigate the organic NLO materials [52–56]. In addition, the polar properties and dipole moment of the title compound were calculated at the B3LYP/6-31+G (d,p) level using Gaussian 03W program package.

Urea is one of the prototypical molecules used is the study of the NLO properties of the molecular systems. Therefore it was used frequently as a threshold value for comparative purposes. The calculated dipole moment and hyperpolarizability values obtained from B3LYP/6-31G method are collected in Table 5.The total molecular dipole moment of 4ACBA from B3LYP with 6-31G (d,p) basis set is 7.9313D which is five times greater than the value for urea (μ_D = 1.3732D). Similarly the first order hyperpolarizability of 4ACBA with B3LYP/6-31+G (d,p) basis set is 3.0539×10^{-30}esu which is greater than the value of urea ($\beta_{tot} = 0.372 \times 10^{-30}$esu). From the computation the high values of the hyperpolarizability of 4ACBA are probably attributed to the charge transfer existing between the phenyl rings within the molecular skeleton. This is evidence for nonlinear optical (NLO) property of the molecule.

ISSN:0975-3583,0976-2833 VOL8,ISSUE04,2017

9.NBO Analysis

Some electron donor orbital, accepter orbital and the interacting stabilization energy resulting from the second- order micro-disturbance theory is reported [40,41].The larger the stabilization energy value, the more intensive is the interaction between electron donors and electron accepters, i.e. the more donating tendency from electron donors to electron acceptors and the grater the extent of conjugation of the whole system. Delocalization of electron density between occupied Lewis-type (bond or lone pair) NBO orbitals and formally unoccupied (anti-bond or Rydberg) non-Lewis NBO orbitals corresponds to a stabilizing donor– accepter interaction.The intramolecular interaction are formed by the orbital overlap between (C–C), *(C–C), (N–C),*(N–C), (C–C), –*(C–C) bond orbital which results intramolecular charge transfer (ICT) causing stabilization of the system.These interactions are observed as increase in electron density (ED) in C– C anti bonding orbital that weakens the respective bonds.These intramolecular charge transfer ($\sigma-\sigma^*$, $\pi-\pi^*$) can induce large nonlinearity of the molecule.

The strong intramolecular hyper conjugation interaction of the r and p electrons of C–C, N–C and C–O to the anti C–C, C–H, N–C and C–O bonds leads to stabilization of some part of the ring as evident from Table 6. NBO analysis has been performed on the molecule at the B3LYP/6-311+G(d,p) level in order to elucidate the intramolecular, re-hybridization and delocalization of electron density within the molecule.For example the intramolecular hyperconjugative interaction of σ (C7–C12) distribute to σ*(C1-C2),(C2-C3),(C3-C4),(C8-C9),(C10-C11) leading to stabilization of 22.76kJ/mol.NBO analysis clearly manifests the evidences of the intra-molecular charge transfer from π (C8–C9) to π*(C7–12) anti-bonding Orbital's as shown in Table 6, that clearly shows stabilization energy of 21.07kJ/mol.The same leads to a strong stabilization energy of 20.56kJ/mol of (C10–C11).

10.NMR ^{1}H and ^{13}C spectral analysis

The isotropic chemical shifts are frequently used as an aid in the identification of reactive organic as well as ionic species.It is recognized that accurate predictions of molecular geometries are essential for reliable calculations of magnetic properties.TheGuage-including atomic orbital (GIAO)[42] ^{1}H and ^{13}C chemical shift calculations of the compound have been made by same method GIAO proocedure is somewhat superior since it exhibits a faster concern of the calculated properties upon extension of the basis set used.Taking in account the computional cost and the effectiveness of calculation,the GIAO method seems to be preferable from many aspects at the present state of thid subject on the other hand,the density functional methodologies offer an effective alternative to the conventional correlated methods, due to their significantly lower computionalcost.The^{1}H and ^{13}C chemical shifts are measured in a less polar (DMSO) solvent.The results in Table.7.shows the range 13_c NMR chemical shift of the typical organic molecule usually is > 100 [43] the accuracy ensures reliable interpretation of spectroscopic parameters.

ISSN:0975-3583,0976-2833 VOL8,ISSUE04,2017

The 13_c NMR chemical shift of C_1 and C_7 are observed larger than carbons whereas their chemical shifts are lower than all other observed.This C_3 and C_4 chemical shifts are determined at 169.324 and 141.895 ppm for 4ACBA.The protons of 4ACBA are observed at 9.149 for H_{21} and at 8.211 for H_{22} ppm respectively.

Another important aspect is that hydrogen attached or near by an electron withdrawing atom or group can decrease the shielding and move the resonance of attached proton towards to higher frequency.By contrast electron donating atom or group increases the shielding and moves the resonance towards to a lower frequency.Electronegative atoms such as nitrogen ,oxygen and halogens deshield hydrogens. The extent deshielding is proportional to the electronegativity of the hetero atom and its proximity to the hydrogen.Electrons on an aromatic ring,double bonded atoms , and triple bonded atoms deshield attached hydrogens.The two oxygen atoms of 4ACBA show electronegative property. The presence of electronegative atom attracts all electron clouds of carbon atoms towards them of carbon atom and net result is increase in chemical shift.Also the chemical shifts obtained and calculated for the hydrogen atoms are quite low are due to shielding effect.The oxygen atoms i.e more electronegative property polarizes the electron distribution in its bond and decreases the electron density of the compounds.

Conclusion

The investigation of the present work, the compute vibrational and molecular structure analysis has been performed based on the quantum mechanical approach by B3LYP/6-31+G(d,p) andHF/6-31+G(d,p)calculations.On the basis of the calculated and experimental results assignment of the fundamental frequencieswere examined. The available experimental results were comparedwith theoretical data. The optimized geometry is tabulated in comparison with the experimental XRD data and well discussed. The electric dipole moment, polarizabilities and the hyperpolarizabilities of the compound have been calculated by B3LYP/6-31+G(d,p) and HF/6-31+G(d,p) method. NLO properties of the 4ACBAaremuch greater than those of urea.NBO analysis was made and it is indicating the intramolecular charge transfer between the bonding and antibonding orbitals. Orbital energy interactionsbetween selective functional groups were analyzed by density of energy states.TheMulliken charges and natural atomic charges of the title molecule have been studied by both the HF and DFT methods. The calculated normal-mode vibrational frequencies provide thermodynamic properties by the way of statistical mechanics.Theoretical ^{1}H and ^{13}C chemical shift values were reportedand compared with experimental data, showing good agreementfor both ^{1}H and ^{13}C.This study demonstrates that scaled DFT/B3LYPcalculations are a powerful approach for understanding the vibrational spectra of medium sized organic compounds.

References

1. "Diagnostic Criteria for Alcohol Abuse and Dependence - Alcohol Alert No. 30-1995".Archived from the original on 27 March 2010. Retrieved 17 April 2010.

ISSN:0975-3583,0976-2833 VOL8,ISSUE04,2017

2. Jump up to:[a] [b] Kahan, M. (Apr 1996). "Identifying and managing problem drinkers". *Can Fam Physician* **42**: 661–71.PMC 2146411. PMID 8653034.
3. Mezler M., Müller T., Raming K. (February 2001). "Cloning and functional expression of GABA(B) receptors from Drosophila". *Eur. J. Neurosci.* **13** (3): 477–486. doi:10.1046/j.1460-9568.2001.01410.x. PMID 11168554.
4. Dzitoyeva S., Dimitrijevic N., Manev H. (April 2003). "Gamma-aminobutyric acid B receptor 1 mediates behavior-impairing actions of alcohol in Drosophila: adult RNA interference and pharmacological evidence". *Proc. Natl. Acad. Sci. U.S.A.***100** (9): 5485–
5490. Bibcode:2003PNAS..100.5485D.doi:10.1073/pnas.0830111100. PMC 154371. PMID 12692303.
5. Bexis S., Phillis B. D., Ong J., White J. M., Irvine R. J. (2004-04-09). "Baclofen prevents MDMA-induced rise in core body temperature in rats". *Drug and Alcohol Dependence* **74** (1): 89–96. doi:10.1016/j.drugalcdep.2003.12.004.PMID 15072812.
6. A.D. Becke, J. Chem. Phys. 98 (1993) 5648–5652.
7. C. Lee, W. Yang, R.G. Parr, Phys. Rev. B 37 (1988) 785–789.
8. B. Miehlich, A. Savin, H. Stoll, H. Preuss, Chem. Phys. Lett. 157 (1989)200-206.
9. M.J. Frisch, G.W. Trucks, H.B. Schlegel et al., Gaussian 03, Revision A.1,Gaussian, Pittsburgh.PA.USA.2003.
10. M.J. Frisch, G.W. Trucks, H.B. Schlegel, G.E. Scuseria, M.A. Robb, J.R. Cheeseman,B. Johnson, W.M. Chen, W. Wong, C. Gonzalez, J.A. Pople, Gaussian, Inc.,Wallingford, CT, 2004.
11. H.B. Schlegel, J. Comput. Chem. 3 (1982) 214–218.
12. E.D. Glendening, A.E. Reed, J.E. Carpenter, F. Weinhold, NBO Version 3.1.
13. TCI,University of Wisconsin, Madison, 1998.
14. A. Frish, A.B. Nielsen, A.J. Holder, Gauss View User Manual, Gaussian Inc.,Pittsburgh, PA, 2001.
15. Gaussian 03 Program, Gaussian Inc., Wallingford, CT, 2004.
16. I.H. Grebogi, A.U.V. Tibola, A. Barison, C.W.P.S. Grandizoli, H.G. Ferraz, L.N.C.
17. Rodrigues, J. Incl. Phenon. Marcocycl. Chem. 10 (1007) (2011) 3.
18. www.Chemcraft.com.
19. Bellamy L J 1980 The infrared spectra of complex molecules (London: Chapman and Hall) vol 2
20. A. Prabakaran, S. Muthu, Spectrochim. Acta A 99 (2012) 90–96.
21. Wiberg K B and Sharke A 1973 SpectrochimActa A29 583
22. V.K. Rastogi, M.A. Palafox, R.P. Tanwar, L. Mittal, Spectrochim. Acta A 58 (2002)1987–2004.
23. M. Silverstein, G.C. Basseler, C. Morill, Spectrometric Identification of OrganicCompounds, Wiley, New York, 1981.
24. L.J. Bellamy, The Infrared Spectra of Complex Molecules, third ed., Wiley, NewYork, 1975.
25. L.J. Bellamy, The Infrared Spectra of Complex Molecules, third ed., Wiley, NewYork, 1975.

ISSN:0975-3583,0976-2833 VOL8,ISSUE04,2017

26. G. Varsanyi, Assignmnet of Vibrational Spectra of Seven Hundred BenzeneDerivatives, vols. 1–2, Adam Hilgler, 1974.
27. N.B. Colthup, L.H. Daly, S.E. Wiberley, Introduction to Infrared and RamanSpectroscopy, Academic Press, New York, 1990.
28. S. Muthu, E.I. Paulraj, Solid State Sci. 14 (2012) 476–487.
29. D. Sajan, J. Binoy, B. Pradeep, K.V. Krishna, V.B. Kartha, I.H. Joe, V.S. Jayakumar,Spectrochim. Acta A 60 (2004) 173–180.
30. GunasekaranS,Seshadri S &MuthuS,*Indian J Pure &Appl Phys*,43.503(2005)
31. GunasekaranS ,Sankari G,&PonnusamyS,*Spectrochim Acta*,61A(2005)117
32. R. Meenakshi, Mol. Simulat. 36 (6) (2010) 425.
33. M. Alcolea Palafox, Int. J. Quantum Chem. 77 (2000) 661–684.
34. X. Sun, Q.L. Hao, W.X. Wei, Z.X. Yu, D.D. Lu Wang, Y.S. Wang, Mol. Struct.THERMOCHEM. 74 (2009) 901–904.
35. P. Politzer, F.A. Awwad, Theor. Chem. Acc. 99 (1998) 83–87.
36. Y.X. Sun, Q.L. Hao, Z.X. Yu, W.X. Wei, L.D. Lu, X. Wang, Mol. Phys. 107 (2009)223.
37. A.B. Ahmed, H. Feki, Y. Abid, H. Boughzala, C. Minot, A. Mlayah, J. Mol. Struct.920 (2009)1.
38. J.P. Abraham, D. Sajan, V. Shettigar, S.M. Dharmaprakash, N.I.H. Joe, V.S.Jayakumar, J. Mol. Struct. (2009) 917–927.
39. S.G. Sagdinc, A. Esme, Spectrochim. Acta A 75 (2010) 1370–1376.
40. A.B. Ahamed, H. Feki, Y. Abid, H. Boughzala, C. Monit, Spectrochim. Acta A 75(2010) 293–298.
41. P. Pulay, G. Fogarasi, G. Ponger, J.E. Boggs, A. Vargha, J. Am. Chem. Soc. 105(1983) 7073–7078.
42. G. Fogarasi, X. Zhou, P.W. Taylor, P. Pulay, J. Am. Chem. Soc. 114 (1992) 8191–8201.
43. B.Osmialowski,E.Kolehmainen,R.Gawinencki, Magn,Reson.chem.29(2001) 334-340
44. R.Marek,J.Brus, J.Tousk, L.kovacs,D.Hockova,Magn.Reson chem.40(2002)353-360
45. Vasanthy M and M. Jeganathan. 2007. Ambient air quality in terms of NOx in and around Ariyalur, Perambalur DT, Tamil Nadu. Jr. of Industrial pollution Control., 23(1):141-144.
46. Vasanthy. M ,A.Geetha, M. Jeganathan,and A.Anitha. 2007. A study on drinking water quality in Ariyalur area. J.Nature Environment and Pollution Technology. 8(1):253-256.
47. Ramanathan R ,M. Jeganathan, and T. Jeyakavitha. 2006. Impact of cement dust on azadirachtain dicaleaves – ameasure of air pollution in and Around Ariyalur. J. Industrial Pollution Control. 22 (2): 273-276.
48. Vasanthy M and M. Jeganathan. 2007. Ambient air quality in terms of NOx in and around Ariyalur, Perambalur DT, Tamil Nadu. Pollution Research., 27(1):165-167.
49. Vasanthy M and M. Jeganathan. 2008.Monitoring of air quality in terms of respirable particulate matter – A case study. Jr. of Industrial pollution Control.,24(1):53 - 55.

ISSN:0975-3583,0976-2833 VOL8,ISSUE04,2017

50. Vasanthy M, A.Geetha, M. Jeganathan, and M. Buvaneswari. 2008. Phytoremediation of aqueous dye solution using blue devil (Eichhornia crassipes). J. Current Science. 9 (2): 903-906.
51. Raajasubramanian D, P. Sundaramoorthy, L. Baskaran, K. Sankar Ganesh, AL.A. Chidambaram and M. Jeganathan. 2011. Effect of cement dust pollution on germination and growth of groundnut (*Arachis hypogaea* L.). IRMJ-Ecology. International Multidisciplinary Research Journal 2011, 1/1:25-30 : ISSN: 2231-6302: Available Online: http://irjs.info/.
52. Raajasubramanian D, P. Sundaramoorthy, L. Baskaran, K. Sankar Ganesh, AL.A. Chidambaram and M. Jeganathan. 2011. Cement dust pollution on growth and yield attributes of groundnut. (*Arachis hypogaea* L.). IRMJ-Ecology. International Multidisciplinary Research Journal 2011, 1/1:31-36.ISSN: 2231-6302. Available Online: http://irjs.info/
53. Jeganathan M, K. Sridhar and J.Abbas Mohaideen. 2012. Analysis of meterological conditions of Ariyalur and construction of wind roses for the period of 5 years from January 2002. J.Ecotoxicol.Environ.Monit., 22(4): 375-384.
54. Sridhar K, J.Abbas Mohaideen M. Jeganathan and P Jayakumar. 2012. Monitoring of air quality in terms of respirable particulate matter at Ariyalur, Tamilnadu. J.Ecotoxicol.Environ.Monit., 22(5): 401-406.
55. Jeganathan M, K Maharajan C Sivasubramaniyan and A Manisekar. 2014. Impact of cement dust pollution on floral morphology and chlorophyll of *healianthus annus* plant – a case study. J.Ecotoxicol.Environ.Monit., 24(1): 29-34.
56. Jeganathan M, C Sivasubramaniyan A Manisekar and M Vasanthy. 2014. Determination of cement kiln exhaust on air quality of ariyalur in terms of suspended particulate matter – a case study. IJPBA. 5(3): 1235-1243. ISSN:0976-3333.
57. Jeganathan M, S Gunaselvi K C Pazhani and M Vasanthy. 2014. Impact of cement dust pollution on floral morphology and chlorophyll of *healianthus annus.*plant a case study. IJPBA. 5(3): 1231-1234. ISSN:0976-3333.
58. Gunaselvi S, K C Pazhani and M. Jeganathan. 2014. Energy conservation and environmental management on uncertainty reduction in pollution by combustion of swirl burners. J. Ecotoxicol. Environ.Monit., 24(1): 1-11.
59. Jeganathan M, G Nageswari and M Vasanthy. 2014. A Survey of traditional medicinal plant of Ariyalur District in Tamilnadu. IJPBA. 5(3): 1244-1248. ISSN:0976-3333.
60. Premalatha P, C. Sivasubramanian, P Satheeshkumar, M. Jeganathan and M. Balakumari.2015. Effect of cement dust pollution on certain physical and biochemical parameters of castor plant (*ricinus communis*). IAJMR.1(2): 181-185.ISSN: 2454-1370.
61. Premalatha P, C. Sivasubramanian, P Satheeshkumar, M. Jeganathan and M. Balakumari.2015. Estimation of physico-chemical parameters on silver beach marine water of cuddalore district. Life Science Archives. 1(2): 196-199.ISSN: 2454-1354.
62. Seshadri V, C. Sivasubramanian P. Satheeshkumar M. Jeganathan and Balakumari.2015. Comparative macronutrient, micronutrient and biochemical constituents analysis of *arachis hypogaea.* IAJMR.1(2): 186-190.ISSN: 2454-1370.
63. Seshadri V, C. Sivasubramanian P. Satheeshkumar M. Jeganathan and Balakumari.2015. A detailed study on the effect of air pollution on certain physical

ISSN:0975-3583,0976-2833 VOL8,ISSUE04,2017

and bio chemical parameters of *mangifera indica*plant.Life Science Archives. 1(2): 200-203.ISSN: 2454-1354.

64. Shakila N, C. Sivasubramanian, P. Satheeshkumar, M. Jeganathan and Balakumari.2015. Effect of municipal sewage water on soil chemical composition- A executive summary. IAJMR.1(2): 191-195.ISSN: 2454-1370.
65. Shakila N, C. Sivasubramanian, P. Satheeshkumar, M. Jeganathan and Balakumari.2015. Bacterial enumeration in surface and bottom waters of two different fresh water aquatic eco systems in Ariyalur, Tamillnadu. Life Science Archives. 1(2): 204-207.ISSN: 2454-1354.
66. Ashok J, S. Senthamil kumar, P. Satheesh kumar and M. Jeganathan. 2016. Analysis of meteorological conditions of ariyalur district. Life Science Archives. 2(3): 579-585.ISSN: 2454-1354. DOI: 10.21276/lsa.2016.2.3.9.
67. Ashok J, S. Senthamil Kumar, P. Satheesh Kumar and M. Jeganathan. 2016. Analysis of meteorological conditions of cuddalore district. IAJMR.2 (3): 603-608.ISSN: 2454-1370. DOI: 10.21276/iajmr.2016.2.3.3.
68. Satheesh Kumar P, C. Sivasubramanian, M. Jeganathan and J. Ashok. 2016. South Indian vernacular architecture -A executive summary. IAJMR.2 (4): 655-661.ISSN: 2454-1370. DOI: 10.21276/iajmr.2016.2.3.3.
69. Satheesh Kumar P, C. Sivasubramanian, M. Jeganathan and J. Ashok. 2016. Green buildings - A review. Life Science Archives. 2(3): 586-590.ISSN: 2454-1354. DOI: 10.21276/lsa.2016.2.3.9.
70. Satheesh Kumar P, C. Sivasubramanian, M. Jeganathan and J. Ashok. 2016. Indoor outdoor green plantation in buildings - A case study. IAJMR.2 (3): 649-654.ISSN: 2454-1370. DOI: 10.21276/iajmr.2016.2.3.3.
71. Manikandan R, M. Jeganathan, P. Satheesh Kumar and J. Ashok. 2016. Assessment of ground water quality in Cuddalore district, Tamilnadu, India. Life Science Archives. 2(4): 628-636.ISSN: 2454-1354. DOI: 10.21276/lsa.2016.2.3.9.
72. Manikandan R, M. Jeganathan, P. Satheesh Kumar and J. Ashok. 2016. A study on water quality assessment of Ariyalur district, Tamilnadu, India. IAJMR.2 (4): 687-692.ISSN: 2454-1370. DOI: 10.21276/iajmr.2016.2.3.3.
73. Sethuraman G, M. Jeganathan, P. Satheesh Kumar and J. Ashok. 2016. Assessment of air quality in Ariyalur, Tamilnadu, India. Life Science Archives. 2(4): 637-640.ISSN: 2454-1354. DOI: 10.21276/lsa.2016.2.3.9.
74. Sethuraman G, M. Jeganathan, P. Satheesh Kumar and J. Ashok. 2016. A study on air quality assessment of Neyveli, Tamilnadu, India. IAJMR.2 (4): 693-697.ISSN: 2454-1370. DOI: 10.21276/iajmr.2016.2.3.3.

ISSN:0975-3583,0976-2833 VOL8,ISSUE04,2017

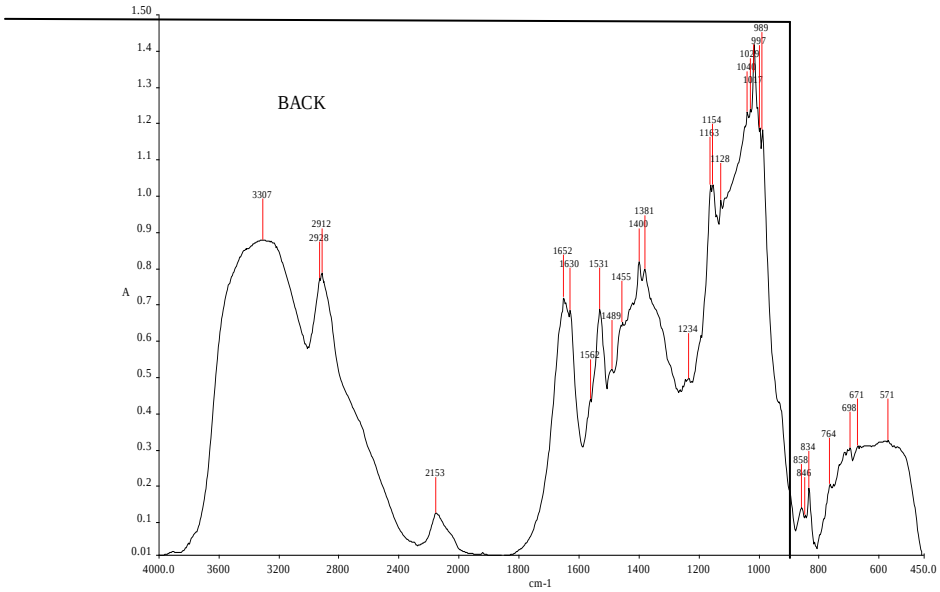

Fig.1. FTIR spectrum of 4ACBA

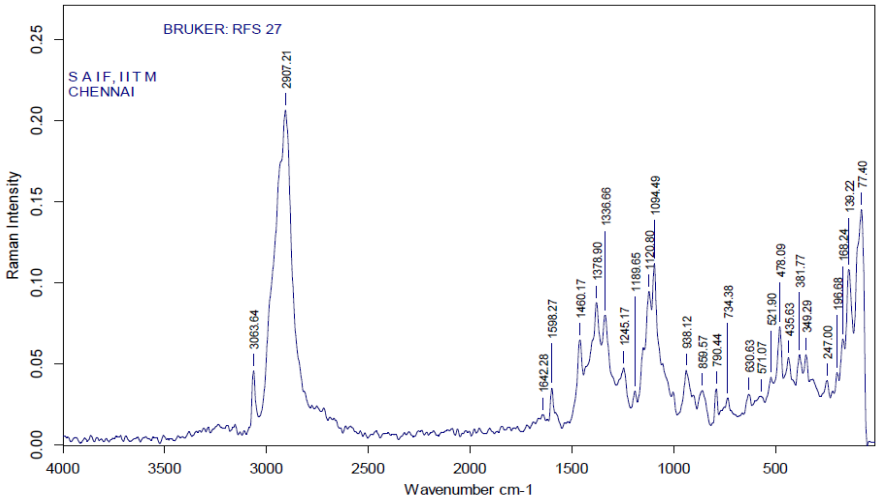

Fig.2. FTRAMAN spectrum of 4ACBA

ISSN:0975-3583,0976-2833 VOL8,ISSUE04,2017

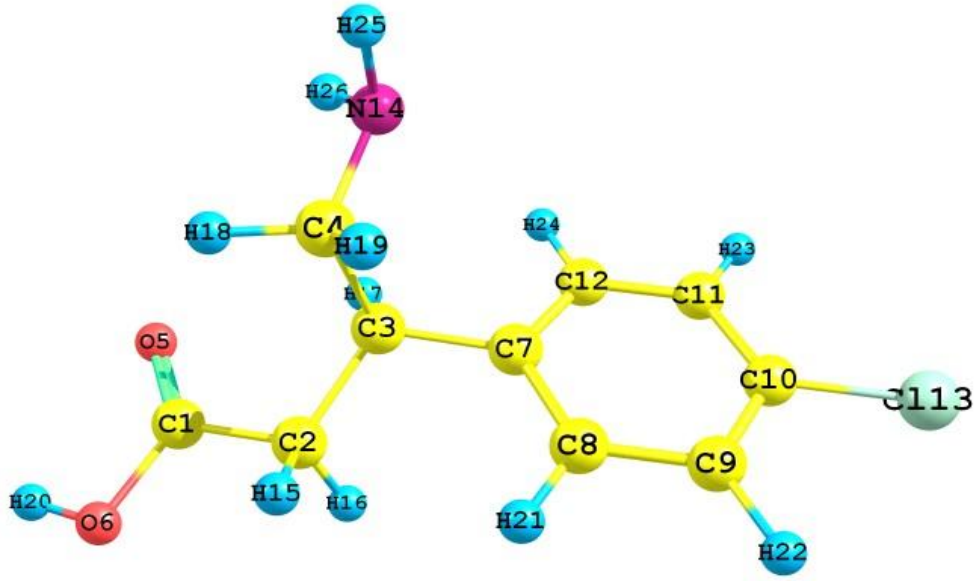

Fig.3. The atom numbering for 4ACBA molecule.

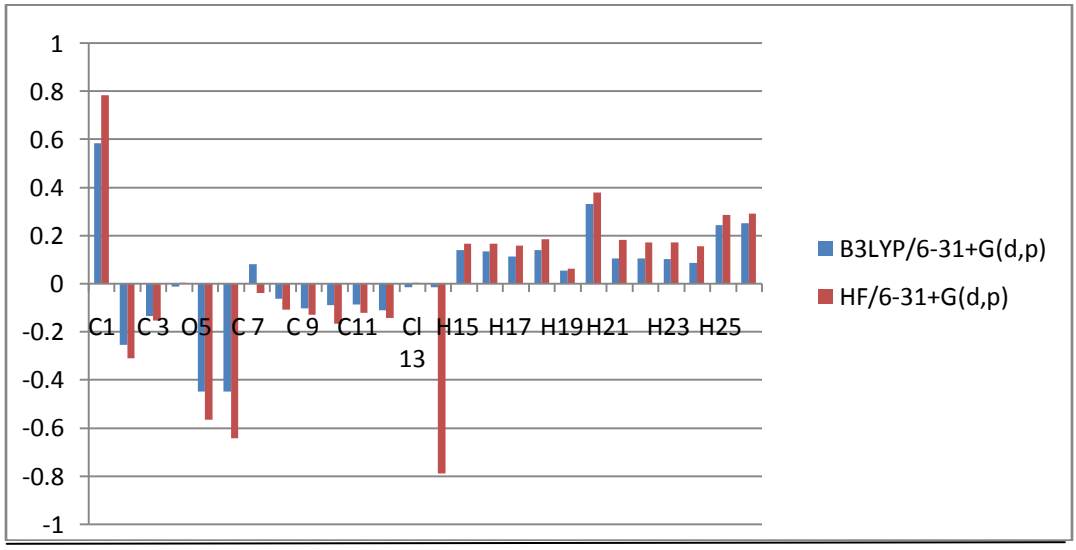

Fig.4. The atom numbering for 4ACBA molecule.

Table.1

Optimized goemetrical parameters of 4ACBA molecule bond length(A) and bond angle (^{o})

ISSN:0975-3583,0976-2833 VOL8,ISSUE04,2017

Bond length

Parameters	B3LYP	HF	Exp
C1-C2	1.515	1.508	1.509
C1-O5	1.212	1.189	1.208
C1-O6	1.355	1.329	1.338
C2-C3	1.537	1.536	1.523
C2-H15	1.096	1.086	1.113
C2-H16	1.097	1.086	1.113
C3-C4	1.55	1.537	1.523
C3-C7	1.52	1.521	1.497
C3-H17	1.096	1.085	1.113
C4-N14	1.464	1.451	1.438
C4-H18	1.102	1.089	1.113
C4-H19	1.097	1.086	1.113
O6-H20	0.972	0.948	0.972
C7-C8	1.401	1.391	1.394
C7-C12	1.401	1.388	1.394
C8-C9	1.396	1.383	1.394
C8-H21	1.086	1.076	1.1
C9-C10	1.394	1.382	1.394
C9-H22	1.084	1.074	1.1
C10-C11	1.394	1.38	1.394
C10-CL13	1.762	1.746	1.719
C11-C12	1.394	1.385	1.394
C11-H23	1.084	1.074	1.1
C12-H24	1.085	1.075	1.1
N14-H25	1.016	1	1.02
N14-H26	1.018	1.001	1.02

Bond angle

Parameters	B3LYP	HF	Exp
C2-C1-O5	126.3	126.2	119.9998
C2-C1-O6	111.3	111.6	120.011
C1-C2-C3	112.9	113.6	109.5001
C1-C2-H15	107.7	107.8	109.4423
C1-C2-H16	106.8	106.2	109.4619
O5-C1-O6	122.4	122.2	120.0002
C1-O6-H20	106.2	108.4	120.0001
C3-C2-H15	112.5	112.2	109.4419

ISSN:0975-3583,0976-2833 VOL8,ISSUE04,2017

C3-C2-H16	110.8	110.6	109.4617
C2-C3-C4	110.7	111.2	109.4999
C2-C3-C7	113.2	111.4	109.4419
C2-C3-H17	106.6	106.9	109.4621
H15-C2-H16	105.6	105.9	109.5195
C4-C3-C7	111.5	112.1	109.4419
C4-C3-H17	106.5	107.2	109.4619
C3-C4-N14	110.6	110.6	109.501
C3-C4-H18	108.5	108.8	109.4419
C3-C4-H19	108.7	109.2	109.4618
C7-C3-H17	108.1	107.7	109.5196
C3-C7-C8	122.3	121.6	119.9985
C3-C7-C12	119.8	120.5	119.9986
N14-C4-H18	113.5	112.9	109.4417
N14-C4-H19	108.3	108.2	109.4618
C4-N14-H25	110.3	111.1	120.0002
C4-N14-H26	109.4	110.6	120.0001
H18-C4-H19	107.1	107.1	109.5201
C8-C7-C12	117.9	117.9	120.0028
C7-C8-C9	121.5	121.5	119.997
C7-C8-H21	120.3	120.2	120.0011
C7-C12-C11	121.5	121.5	119.9995
C7-C12-H24	119.2	119.6	120.0003
C9-C8-H21	118.2	118.3	120.0019
C8-C9-C10	119.1	119.2	120.0002
C8-C9-H22	120.7	120.6	119.9999
C10-C9-H22	120.2	120.1	119.9999
C9-C10-C11	120.9	120.7	120.0033
C9-C10-CL13	119.5	119.6	119.9983
C11-C10-CL13	119.6	119.7	119.9984
C10-C11-C12	119.1	119.2	119.9972
C10-C11-H23	120.1	120.2	120.0016
C12-C11-H23	120.7	120.6	120.0012
C11-C12-H24	119.3	118.9	120.0002
H25-N14-H26	106.4	107.4	119.9997

ISSN:0975-3583,0976-2833 VOL8,ISSUE04,2017

Table.2 Vibrational assignment of Baclofen

S. no.	Observed wavenumber(cm^{-1})		Calculated wavenumber(cm^{-1})									Vibrational assignments
			PM-6			HF/6-31+G(d,p)			B3LYP/6-31+G(d,p)			
	FTIR	FT-RAMAN	Unscaled	Scaled	IR intensity	Unscaled	Scaled	IR intensity	Unscaled	Scaled	IR intensity	
1	3307		2839	3620	48.85	4127	3590	137.78	3751	3308	53.31	$\upsilon_s(NH_2)$(99)
2		3275	2802	3435	70.40	3834	3340	1.96	3581	3278	0.441	$\upsilon_{as}(NH_2)$(99)
3		3198	2760	3420	2.09	3745	3280	1.029	3494	3199	0.21	$\upsilon_s(CH_2)_2$ (99)
4		3063	2753	3229	353.46	3383	3124	2.777	3221	3065	3.157	$\upsilon_s(CH_2)_2$ (99)
5	2975	2978	2746	3108	3.63	3382	3052	9.30	3218	2979	6.39	$\upsilon_{as}(CH_2)_2$ (99)
6	2948		2744	3090	88.31	3355	3003	11.075	3205	2950	4.82	$\upsilon_{as}(CH_2)_2$ (100)
7	2928		2734	3013	68.38	3346	2933	16.49	3188	2931	12.39	$\upsilon_s(CH_2)$ (95)
8	2912		2726	2980	30.74	3252	2874	18.37	3091	2915	10.46	$\upsilon_s(CH_2)$ (51)
9		2907	2674	2940	65.11	3235	2820	21.86	3072	2911	30.5	υ(CH) (82)
10		2736	2652	2870	50.95	3215	2020	22.96	3056	2742	6.23	$\upsilon_{as}(CH_2)_2$ (97)
11	1652		2649	2000	50.74	3209	2005	8.18	3052	1657	3.23	$\upsilon_{as}(CH_2)_2$ (100)
12		1642	2546	1955	382.24	3160	1983	82.15	2985	1648	80.8	υ(OH) (98)
13	1630		1833	1872	418.97	2021	1885	350.26	1837	1637	228	υ(OC)(86)
14	1489		1642	1620	0.74	1807	1723	21.14	1668	1494	28.25	CCC bending (12),υ (CC)(56)
15		1460	1638	1580	7.82	1806	1695	25.77	1652	1465	6.41	υ(CC)(81)
16	1455		1612	1530	13.86	1769	1543	0.097	1626	1460	0.26	HNH bending(78),torHNCC(21)
17		1437	1509	1495	91.52	1670	1482	65.19	1536	1442	61.2	υ(CC)(22),CCC bending(15),HCC bending(43)
18		1413	1466	1456	3.86	1643	1473	2.82	1514	1418	5.10	υ(CC)(45)
19	1400		1350	1432	56.35	1596	1325	44.85	1474	1406	18.21	υ(CC)(29)
20	1381		1330	1399	39.25	1581	1280	58.57	1452	1386	14.2	HCN bending(12), HNC bending(12)
21		1378	1326	1387	290.2	1567	1004	14.95	1426	1382	64.90	υ (CC)(16),υ(OC)(17),HCCOtor(12)
22		1336	1305	1362	6.67	1558	1365	55.06	1424	1342	34.05	HCH bending(17), HCCC tor(21)
23		1261	1292	1302	24.23	1499	1320	14.32	1377	1267	19.35	HCC bending (81)
24		1245	1270	1291	21.17	1479	1293	21.10	1358	1252	4.75	υ(NC)(12),tor HCCC
25	1234		1258	1273	95.8	1445	1284	8.69	1350	1240	8.26	υ(NC)(10)
26		1189	1254	1201	19.40	1436	1255	7.63	1333	1195	0.97	υ(OC)(12),HOC bending(17),HCH bending(22)
27	1154		1241	1184	6.80	1404	1208	11.37	1323	1162	3.77	υ(NC)(10),HCC bending(25)
28	1128		1229	1153	44.88	1371	1193	21.60	1280	1135	15.63	HCC bending(13), HCH bending(26)
29		1120	1221	1137	13.55	1321	1180	29.7	1225	1129	15.22	HCC bending(14), HCH bending(26), υ(CC)(13)
30		1094	1218	1122	6.18	1303	1152	49.34	1216	1108	1-86	HCC bending(70), HCC bending(13)
31		1054	1216	1111	28.6	1299	1145	162	1213	1063	1.95	HCH bending(21)
32	1040		1167	1084	15.74	1269	1131	69	1167	1049	157	υ(CC)(11), HCC bending(70)
33	1039		1162	1065	10.95	1246	1125	3.24	1157	1046	75.47	υ(CC)(39), tor HCCO (11)
34		1019	1147	1053	18.87	1205	1118	57.1	1140	1025	48.96	υ(CC)(41), HCC bending(11),HCN bending(12)
35	997		1124	1020	63.02	1195	1095	27.14	1111	1008	57.35	HCN bending(11)
36	989		1106	999	70.01	1190	1072	2.18	1101	996	16.19	υ(OC)(11),HOC bending(12), υ(CC)14)
37		938	1076	953	26.3	1156	1068	2.67	1083	947	6.93	HCC bending(25)
38		914	1069	932	9.95	1117	1035	2.84	1037	928	3.83	υ(CC)(25), HCC bending(11)
39		875	1033	903	103.2	1108	1029	22.6	1027	886	28.67	HNCC tor(24)
40	858	859	1005	897	85.9	1097	1000	0.23	1003	871	1.95	υ(CC)(31), υ(OC)(15)
41	846		993	873	90.8	1090	983	5.51	962	852	0.048	υ(CC)(20)
42	834		971	854	0.44	1079	957	0.7910	954	843	0.13	HCCC tor(81)
43		791	963	800	0.17	980	933	29.87	902	808	26.8	HCCC tor(81),CCCC tor(35)
44		787	921	793	67.5	951	910	43.28	872	797	35.87	CCCbending(20)
45	764		888	785	44.6	940	902	0.66	847	775	86	υ(CC)(17),out OCOC(12),HCCOtor(45)
46		755	879	778	1.07	932	898	20	834	762	12	HCCC tor(97)
47		734	867	753	74.6	917	895	120.62	833	743	16	HCCC tor(72)
48	698		833	724	19.35	852	862	7.67	793	708	9.5	CCC bending(22),υ(HLC)(11)
49	671	668	695	701	32.23	805	803	3.84	729	675	4.18	CCC bending(20),
50		630	670	683	3.97	747	798	34.98	688	641	29.21	HCCC tor(11), CCCC out(18), CCCC tor(15)

ISSN:0975-3583,0976-2833 VOL8,ISSUE04,2017

51		583	607	620	5.82	714	783	118	681	593	97	CCC bending(48)
52	571	571	601	595	92.01	698	780	0.625	650	585	0.15	HOCC tor(24),OCOC out(36)
53		521	566	572	68.54	664	772	41.7	611	532	21.20	OCO bending(35), HOCC tor(39),
54		484	547	500	40.92	630	695	52.86	580	493	52.44	CCC bending(10),CLCC out,HCCC 478tor(10)
55		478	512	495	3.03	580	623	22	543	486	18.39	CCC bending(13),CCCC out(24)
56		436	491	463	14.26	558	587	11.64	523	448	7.90	HOCC tor(22),OCO bending(23)
57		421	466	433	18.16	507	473	15.83	454	432	18.87	NCC bending(16),OCOC out(11),CCC bending(10)
58		381	395	403	14.02	459	405	0.02	419	393	0.16	CCC bending(12),NCC bending(19)
59		372	354	398	0.10	432	385	6.08	397	384	3.33	HCCC tor(21), CCCC out(39),
60		349	346	385	2.61	383	373	2	360	360	2.16	OCC bending(40),CCCbending(12)
61		334	322	329	3.77	368	352	1.17	345	434	0.96	CLCC bendind(48)
62		318	298	333	1.41	319	349	3.08	283	332	4.48	CLCC bendind(12),CCCC tor(15),CLCCC out(20)
63		290	260	305	62.4	261	323	24.5	246	310	25.78	HNCC tor(81)
64		265	209	286	2.07	227	315	0.618	227	284	0.47	NCC bending(10)
65		265	178	273	2.61	217	296	17.25	206	261	9.45	CLCC bending(11), OCC bending(11), CCC bending(47)
66		247	166	225	2.49	204	286	3.83	198	218	6.36	CCC bending(12)
67		196	127	203	0.87	152	262	1.72	152	181	1.16	CCC bending(30), CCCC tor(12)
68		168	65	195	0.84	86	224	1.85	85	155	1.00	NCC tor(16)
69		139	49	158	1.38	77	197	0.80	78	140	1.71	CCCC tor(24), CCC bending(17),CCCC tor(42)
70		128	33	124	1.25	55	163	0.74	51	121	0.33	CCCC tor(12)
71		97	25	101	0.25	47	124	0.57	41	92	0.58	CCCC tor(61),CCCC out(10)
72		77	19	84	1.18	28	93	0.23	22	63	0,31	OCCC tor(74)

Table 3.
Natural atomic charges of 4ACBA

Atom with numbering	MPA		NPA	
	B3LYP/6-31+G(d,p)	HF/631+G(d,p)	B3LYP/6-31+G(d,p)	HF/631+G(d,p)
C1	0.584774	0.783885	0.8387	1.00173
C2	-0.255385	-0.310189	-0.55639	-0.53653
C 3	-0.135015	-0.152965	-0.28118	-0.26353
C 4	-0.011921	0.004746	-0.26368	-0.21403
O5	-0.447635	-0.567156	-0.61378	-0.72039
O6	-0.447635	-0.642497	-0.72425	-0.80811
C 7	0.081537	-0.038927	-0.04863	-0.05069
C 8	-0.063494	-0.107226	-0.21596	-0.20848
C 9	-0.101423	-0.129237	-0.242	-0.23213
C10	-0.089544	-0.165485	-0.06994	-0.06237
C11	-0.085914	-0.121687	-0.24504	-0.23521
C12	-0.109794	-0.142134	-0.22529	-0.22011
Cl 13	-0.015369	0.003575	0.01307	-0.00793
N14	-0.015369	-0.790867	-0.95433	-0.99946

ISSN:0975-3583,0976-2833 VOL8,ISSUE04,2017

H15	0.138544	0.165819	0.26955	0.25807
H16	0.135527	0.165326	0.27205	0.26049
H17	0.112422	0.15719	0.26843	0.25712
H18	0.140568	0.184567	0.26409	0.26093
H19	0.055812	0.063122	0.1854	0.16992
H20	0.331163	0.380597	0.51838	0.53961
H21	0.10559	0.181349	0.25356	0.25162
H22	0.104276	0.172851	0.25376	0.25062
H23	0.103563	0.171871	0.25361	0.25037
H24	0.087026	0.156847	0.24218	0.23801
H25	0.244385	0.285166	0.40392	0.40987
H26	0.251178	0.29146	0.40375	0.41061

Table 4.

Theoretically computed energies (a.u), zero-point vibrational energies (kcal mol1), rotational constants (GHz), entropies (cal mol1), dipole moment (D), heat capacity (kcal mol1 K1) and rotational temperature (K).

Parameter	HF/6-31+G(d,p)	B3LYP/6-31+G(d,p)
Zero point vibrational energy(Kcal/Mol)	140.634	130.955
Gibbs free energy	0.18198	0.16564
zero point correction	0.22411	0.2086
Thermal free energy	-1049.189	-1053.55
Rotational constant (GHz)	1.31074	1.33966
	0.25203	0.24971
	0.23295	0.22572
Rotational temperatures (Kelvin)	0.06291	0.06429
	0.0121	0.01198
	0.01118	0.01083
Dipole moment		
μ_x	2.1172	-3.2354
μ_y	-0.9433	-0.1847
μ_z	-0.5955	1.0646
μ_{total}	2.3931	3.4111
Entropy (Cal/Mol-Kelvin)		
Total	118.218	121.727
Translational	41.973	47.973

ISSN:0975-3583,0976-2833 VOL8,ISSUE04,2017

Rotational	32.702	32.721
Vibrational	43.544	47.034
Energy (KCal/Mol)		
Total	148.848	139.647
Translational	0.889	0.889
Rotational	0.889	0.889
Vibrational	147.071	137.869
Molar capacity at constant volume (Cal/Mol-Kelvin)		
Total	47.442	50.901
Translational	2.981	2.981
Rotational	2.981	2.981
Vibrational	41.48	44.939

Table 5.
The values of calculated dipole moment (μD), polariazability (α_0), first hyperpolarizability (β_{tot}) components of 4ACBA

Parameters	B3LYP/6-31G(d,p)	Parameters	B3LYP/6-31G(d,p)
μ_x	0.4605	β_{xxx}	-116.395
μ_y	0.7573	β_{xxy}	42.08
μ_z	0.2861	β_{xyy}	123.475
μ_D	7.9313	β_{yyy}	280.05
α_{xx}	140.43	β_{xxz}	86.53
α_{xy}	32.433	β_{xyz}	48.44
α_{yy}	151.3098	β_{yyz}	35.882
α_{xz}	-9.470	β_{xzz}	-49.02
α_{yz}	-8.0122	β_{yzz}	-26.223
α_{zz}	83.728	β_{zzz}	65.16
α_o (esu)	1.8546×10^{-23}	β_{tot} (esu)	3.0539×10^{-30}
Δα (esu)	3.919×10^{-23}		

ISSN:0975-3583,0976-2833 VOL8,ISSUE04,2017

Table 6.
Second order perturbation theory analysis of fock matrix in NBO basis.

Donor (i)	Type	ED(e)	Acceptor(j)	Type	ED(e)	E(2)a (kJ/mol)	E(j) - E(i)b (a.u.)	F(i, j)c (a.u.)
C1-C2	σ	1.9798	C1-O5	σ *	0.2167	0.62	1.27	0.025
			C2-C3	σ *	0.0196	0.53	1.04	0.021
			C3-C7	σ *	0.0299	1.92	1.11	0.041
			O6-H20	σ *	0.0146	3.22	1.08	0.053
C1-O5	σ	1.9971	C1-C2	σ *	0.0567	0.99	1.47	0.034
C1-O5	π	1.9883	C1-O5	π*	0.2167	0.87	0.39	0.017
			C2-H15	σ *	0.0139	1.5	0.79	0.031
			C2-H16	σ *	0.0117	1.38	0.8	0.03
			C4-H18	σ *	0.0316	1.19	0.86	0.029
C1-O6	σ	1.9971	C2-C3	σ *	0.0196	0.66	1.36	0.027
C2-C3	σ	1.9629	C1-C2	σ *	0.0567	0.83	0.99	0.026
			C1-O6	σ *	0.0927	4.44	0.98	0.06
			C2-H15	σ *	0.0139	0.59	1.02	0.022
			C2-H16	σ *	0.0117	0.64	1.02	0.023
			C3-C4	σ *	0.0185	0.86	1.01	0.026
			C3-C7	σ *	0.0299	1.29	1.05	0.033
			C3-H17	σ *	0.0231	0.62	1.04	0.023
			C4-N14	σ *	0.0082	2.1	1.03	0.043
			C7-C8	σ *	0.0246	0.74	1.19	0.027
			C7-C12	σ *	0.3492	2.56	0.65	0.04
C2-H15	σ	1.9673	C1-O5	σ *	0.0242	1.66	1.12	0.039
			C1-O5	σ *	0.2167	4.79	0.51	0.047
C2-H16	σ	1.9672	C1-05	σ *	0.0242	1.85	1.12	0.041
			C1-05	σ *	0.2167	4.5	0.51	0.045
			C2-C3	σ *	0.0196	0.54	0.89	0.02
			C3-C4	σ *	0.0185	2.98	0.91	0.047
C3-C4	σ	1.9379	C2-C3	σ *	0.0196	0.89	0.97	0.026
			C2-H16	σ *	0.0117	1.87	1	0.039
			C3-H17	σ *	0.0231	0.73	1.02	0.024
			C4-H18	σ *	0.0316	0.77	1.07	0.026
			C7-C12	σ *	0.3492	3.04	1.17	0.053
			N14-H25	σ *	0.0061	2.6	1.08	0.048
C3-C7	σ	1.9682	C1-C2	σ *	0.0567	2.14	1	0.042
			C2-C3	σ *	0.0196	1.32	1.01	0.033
			C3-C4	σ *	0.0185	1.07	1.02	0.03
			C3-H17	σ *	0.0231	0.64	1.05	0.023
			C4-H18	σ *	0.0316	1.41	1.1	0.035

ISSN:0975-3583,0976-2833 VOL8,ISSUE04,2017

			C7-C8	σ *	0.0246	2.55	1.21	0.05
			C7-C12	σ *	0.3492	2.41	1.21	0.049
			C8-C9	σ *	0.3235	2.15	1.21	0.046
			C11-C12	σ *	0.0151	2.14	1.2	0.045
C3-H17	σ	1.9673	C2-H15	σ *	0.0139	2.81	0.89	0.045
			C3-C4	σ *	0.0185	0.51	0.88	0.019
			C3-C7	σ *	0.0299	0.66	0.93	0.022
			C4-H19	σ *	0.0364	2.68	0.92	0.044
			C7-C12	σ *	0.3492	3.09	1.07	0.051
C4-N14	σ	1.9937	C2-C3	σ *	0.0196	1.88	1.1	0.041
			C3-C4	σ *	0.0185	0.51	1.11	0.021
C4-H18	σ	1.9816	C3-C4	σ *	0.0185	0.71	0.87	0.022
			C3-C7	σ *	0.0299	2.91	0.92	0.046
			N14-H26	σ *	0.0088	1.89	0.96	0.038
C4-H19	σ	1.9792	C3-H17	σ *	0.0231	3.06	0.91	0.047
			C8-H21	σ *	0.0162	1.66	0.94	0.035
			N14-H26	σ *	0.0088	1.63	0.98	0.036
O6-H20	σ	1.9883	C1-C2	σ *	0.0567	4.3	1.15	0.064
			C1-O5	σ *	0.02421	0.85	1.39	0.031
C7-C8	σ	1.9726	C3-C7	σ *	0.0299	2.58	1.14	0.048
			C3-H17	σ *	0.0231	0.67	1.12	0.024
			C7-C12	σ *	0.3492	3.96	1.28	0.064
			C8-C9	σ *	0.3235	2.91	1.28	0.055
			C8-H21	σ *	0.0162	1.36	1.15	0.036
			C9-H22	σ *	0.0125	2.17	1.14	0.045
			C12-H24	σ *	0.0131	2.2	1.14	0.045
C7-C12	σ	1.9745	C3-C4	σ *	0.0185	1	1.09	0.029
			C3-C7	σ *	0.0299	2.56	1.14	0.048
			C7-C8	σ *	0.0246	3.99	1.28	0.064
			C8-H21	σ *	0.0162	2.21	1.16	0.045
			C11-C12	σ *	0.01508	2.76	1.27	0.053
			C11-H23	σ *	0.0124	2.22	1.15	0.045
			C12-H24	σ *	0.01311	1.14	1.14	0.032
C7-C12	σ	1.6566	C1-C2	σ *	0.0567	0.74	0.63	0.021
			C2-C3	σ *	0.0196	3.09	0.63	0.043
			C3-C4	σ *	0.0185	0.54	0.65	0.018
			C3-H17	σ *	0.0231	0.69	0.68	0.021
			C8-C9	σ *	0.3235	19.7	0.28	0.067
			C10-C11	σ *	0.3991	22.76	0.27	0.07
C8-C9	σ	1.9729	C3-C7	σ *	0.0299	3.42	1.14	0.056
			C7-C8	σ *	0.0246	3.29	1.28	0.058

ISSN:0975-3583,0976-2833 VOL8,ISSUE04,2017

			C8-H21	σ *	0.0162	1.27	1.16	0.034
			C9-C10	σ *	0.2818	3.08	1.26	0.056
			C9-H22	σ *	0.0125	1.14	1.15	0.032
			C10-CL13	σ *	0.0277	4.57	0.87	0.056
C8-C9	π	1.6643	C7-C12	π*	0.3492	21.07	0.29	0.07
			C10-C11	π*	0.3991	20.56	0.26	0.067
C8-H21	σ	1.9774	C4-H19	σ *	0.03641	0.69	0.95	0.023
			C7-C8	σ *	0.0246	1.44	1.1	0.036
			C7-H12	σ *	0.02326	4.21	1.1	0.061
			C8-C9	σ *	0.0157	0.87	1.1	0.028
			C9-C10	σ *	0.2818	3.7	1.08	0.056
C9-C10	σ	1.9804	C8-C9	σ *	0.3235	2.62	1.3	0.052
			C8-H21	σ *	0.0162	2.11	1.18	0.045
			C9-H22	σ *	0.0125	1.29	1.17	0.035
			C10-C11	σ *	0.3991	4.04	1.28	0.064
			C11-H23	σ *	0.0124	4.24	1.17	0.46
C9-H22	σ	1.9811	C7-C8	σ *	0.0246	3.68	1.1	0.057
			C8-C9	σ *	0.0157	0.94	1.1	0.029
			C9-C10	σ *	0.2818	0.81	1.08	0.027
			C10-C11	σ *	0.3991	3.91	1.08	0.058
C10-C11	σ	1.9803	C9-C10	σ *	0.2818	4.04	1.28	0.064
			C9-H22	σ *	0.0125	2.23	1.17	0.046
			C11-C12	σ *	0.01508	2.62	1.3	0.052
			C11-H23	σ *	0.0124	1.3	1.17	0.035
			C12-H24	σ *	0.01311	2.16	1.16	0.045
C10-C11	σ	1.6851	C7-C12	σ *	0.02326	17.35	0.3	0.065
			C8-C9	σ *	0.0157	19.31	0.3	0.068
C10-CL13	σ	1.9	C8-C9	σ *	0.0157	2.15	1.33	0.048
			C11-C12	σ *	0.01508	2.16	1.32	0.048
C11-C12	σ	1.9733	C3-C7	σ *	0.0299	3.42	1.14	0.056
			C7-C12	σ *	0.02326	3.14	1.28	0.057
			C10-C11	σ *	0.3991	3.05	1.26	0.055
			C10-CL13	σ *	0.0277	4.52	0.87	0.056
			C11-H23	σ *	0.0124	1.12	1.15	0.032
			C12-H24	σ *	0.01311	1.11	1.14	0.032
C11-H23	σ	1.9811	C7-C12	σ *	0.02326	3.57	1.1	0.056
			C9-C10	σ *	0.2818	3.9	1.08	0.058
			C10-C11	σ *	0.3991	0.083	1.08	0.027
			C11-C12	σ *	0.01508	0.85	1.1	0.027
C12-H24	σ	1.9807	C7-C8	σ *	0.0246	4.31	1.1	0.062
			C7-C12	σ *	0.02326	1.15	1.11	0.032

ISSN:0975-3583,0976-2833 VOL8,ISSUE04,2017

			C10-C11	σ *	0.3991	3.66	1.08	0.056
			C11-C12	σ *	0.01508	0.81	1.1	0.027
N14--H25	σ	1.9933	C3-C4	σ *	0.0185	2.15	1.01	0.042
N14-H26	σ	1.9935	C4-H18	σ *	0.0316	0.61	1.09	0.023
			C4-H19	σ *	0.03641	0.8	1.04	0.026
LP(1)O5	σ	1.9713	C1-C2	σ *	0.0567	2.17	1.06	0.043
			C1-O6	σ *	0.0927	0.04	1.06	0.024
			C4-H18	σ *	0.0316	2.79	1.16	0.051
LP(2)O5	π	1.8611	C1-C2	σ *	0.0567	18.16	0.64	0.098
			C1-O6	σ *	0.0927	32.76	0.64	0.13
			C3-C7	σ *	0.0299	0.81	0.71	0.022
			C4-H18	σ *	0.0316	1.65	0.74	0.032
LP(1)O6	σ	1.9739	C1-C2	σ *	0.0567	0.63	0.93	0.022
			C1-O5	σ *	0.2167	8.39	1.16	0.088
LP(2)O6	π	1.8162	C1-O5	π*	0.2167	49.4	0.34	0.117
LP(1)CL13	σ	1.9926	C9-C10	σ *	0.2818	1.47	1.48	0.042
			C10-C11	σ *	0.3991	1.46	1.48	0.042
LP(2)CL13	π	1.9701	C9-C10	σ *	0.2818	4.4	0.88	0.056
			C10-C11	σ *	0.3991	4.44	0.88	0.056
LP(1)N14	σ	1.9421	C4-H18	σ *	0.0316	5.43	0.68	0.055
			C4-H19	σ *	0.03641	7.6	0.64	0.063
			C8-C9	σ *	0.0157	1.09	1.09	0.016

Table.7.

The calculated chemical shift of carbon and hydrogen atoms of 4ACBA

Atoms	Isotropic chemical shielding tensor(ppm)	Shift (ppm)
C_1	30.660	169.324
C_7	58.0894	141.895
C_8	65.279	134.706
C_2	149.488	50.497
C_3	145.253	54.731
H_{21}	23.447	9.149
H_{22}	24.386	8.211
H_{25}	31.407	1.190
H_{26}	31.988	0.609